NUCL SCI TECH (2017) 28:161
DOI 10.1007/s41365-017-0306-8

Injector of the Turkish light source facility TURKAY

Zafer Nergiz[1] · Avni Aksoy[2]

Received: 12 December 2016 / Revised: 2 April 2017 / Accepted: 6 April 2017 / Published online: 26 October 2017

Abstract A synchrotron radiation source called TURKAY is proposed as a sub-project of the Turkish Accelerator Center Project. The storage ring of TURKAY is a low emittance synchrotron and the radiation ranges between 0.01 and 60 keV can be generated from the insertion devices and bending magnets placed on it. The injector system of the facility will mainly consist of a 150 MeV linac and full energy booster. In this study, we present design considerations and beam dynamics studies of the pre-injector linac and booster ring for TURKAY.

Keywords Booster ring · Pre-injector linac · Beam dynamics

1 Introduction

The Turkish Accelerator Center (TAC) is a project aimed to build some accelerator facilities in Turkey, and at first stage, an infrared FEL facility named TARLA is under construction [1–3]. Another part of the TAC is to build a synchrotron radiation facility (TURKAY), and this facility is in a detailed design stage. The storage ring is designed, and the results from the lattice optimization and the radiation properties have been presented in previous studies [4, 5]. The designed storage ring has a 0.51 nm rad emittance at 3 GeV electron energy, and the ring circumference is 477 m. This design is on par with other designs in the world community.

The major task of the injector is to generate and accelerate the electrons to an energy of 3 GeV. Then, the electron beam is extracted from the booster and transferred into the storage ring. A full energy injection system is the solution to reach design performance in an ultra-low emittance ring. A low energy linac with a full energy booster has been the choice for most light source injection systems because of its advantages in cost and reliability. Therefore, the design concept of TURKAY is composed of three parts: Injector, Full Energy Booster Ring, and Storage Ring. The electron bunches generated by the electron gun are accelerated up to 150 MeV in a linear accelerator, and they are injected into a booster synchrotron which raises the beam energy to nominal operation value up to 3 GeV. Then, they are injected into the storage ring. The booster and storage ring RF systems will operate at approximately 500 MHz, and the main reason for that is the availability of RF cavities that can be commercially supplied at this frequency.

2 Design considerations

The storage ring shall have several fill-pattern modes according to user requirements such as uniform filling mode, half fill mode, and hybrid-fill mode. For instance, time-resolved science requires operating modes with a single bunch, full fill or hybrid fills, while diffraction applications require uniform fill pattern. The maximum

This work was supported by the Turkish Republic Ministry of Development (No. DPT2006K120470).

✉ Zafer Nergiz
znergiz@ohu.edu.tr

1 Department of Physics, Faculty of Arts and Sciences, Omer Halisdemir University, 51200 Nigde, Turkey

2 Institute of Accelerator Technologies, Ankara University, 06830 Gölbaşı, Ankara, Turkey

number of bunches in an SR is defined with $N_b = C_{SR}/t_{rep}$ where C_{SR} is the circumference of the storage ring and t_{rep} is the minimum spacing between bunches $t_{rep} = n/f_{RF}$ where f_{RF} is the operating frequency of the RF structure on storage ring and n is the integer.

One of the important operating considerations is the fill-up method of the storage ring. There exist two types of filling methods for a single bunch: refill mode and top-up fill mode. In refill mode, the pattern of bunches is filled to SR in time periods depending on lifetime. In top-up fill mode, stored beam current is maintained at a near constant level using frequent injection [6, 7]. Therefore, the gun and pre-injector should provide a full bunch pattern equivalent to the booster ring circumference and should allow the flexible bunching system. Top-up injection is nowadays state of the art for storage ring-based SR sources. For radiation safety reasons, the electron beam losses during injection with open photon beam shutters have to be minimized. Therefore, the booster emittance should be small to capture the full beam in the storage ring acceptance.

3 Pre-injector linac

The pre-injector linac of TURKAY consists of a 100 kV DC thermoionic gun, a sub-harmonic pre-buncher operating at 500 MHz, a pre-buncher operating at 3 GHz, a standing wave buncher operating at 3 GHz, and two traveling wave accelerating structures operating at 3 GHz, similar to ALBA project [8]. Schematic layout of injector is given in Fig. 1.

The electron gun is the standard triode gun, and it is modulated by a 500 MHz amplifier. Therefore, the beam pulse structure at the gun is already matched to the booster and storage ring RF-bucket structure. After extraction of current from a cathode, the electron bunches can be created with a modulated voltage system at a length of $\sigma_t \approx 1$ ns. The bunches will be compressed down to $\sigma_t \approx 10$ ps in the drift sections by the energy modulation obtained in the sub-harmonic pre-buncher and the buncher. Final energy modulation and bunching will be performed in the buncher cavity in order to reduce the energy spread and to minimize the losses. The bunches will be accelerated to the final energy of 150 MeV by three traveling wave accelerating structures (Table 1).

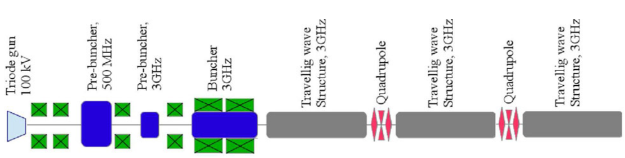

Fig. 1 (Color online) Layout of TURKAY pre-injector linac

Table 1 Beam parameters of the TURKAY injector linac

Parameter	Single bunch	Multi bunch
Energy (MeV)	> 150	> 150
Pulse length (ns)	1	600
Pulse charge (nC)	1	6
RMS emittance (mm mrad)	< 50	< 50
Energy spread (%)	< 1	< 1

ASTRA [9] code has been used to analyze the beam behavior, such as the radial control, the bunching process, the energy spread, emittance, and transmission rate along the pre-injector. In the calculations, we have assumed that the maximum length of a single bunch of 1 nC is 1 ns at the exit of the gun. The longitudinal distribution of bunches have inverted parabolic distribution, and they have a 10 mm mrad emittance at maximum bunch charge.

The evolution of the transverse beam size and emittance from the electron source to the end of the injector is given in Fig. 2. The energy increment, bunch length variation, and beam loss rate along the injector is given with Fig. 3. Final phase spaces and parameters of single bunch are shown in Fig. 4. As it is seen from the figure, the transverse emittance is lower than 50 mm mrad. Figure 3 shows that more than 85% of particles carried to the booster ring and bunch are compressed down to 2 mm. As it can be seen on the figure, almost 15% of the particles are lost in the vacuum chamber between second pre-buncher and buncher cavity and on cavity walls of the initial two cell of the buncher cavity.

4 Booster

Almost all of the synchrotron radiation facilities in operation or in their design process have chosen a full energy booster synchrotron as an injector together with a low energy linac as the pre-injector. Some of the sources that have a booster share the same tunnel with the storage

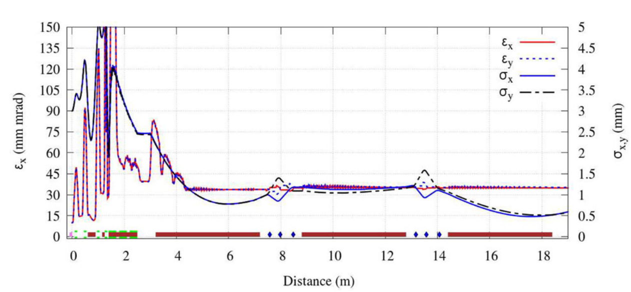

Fig. 2 (Color online) Transverse beam sizes and projected emittance variation of a single bunch along the injector linac

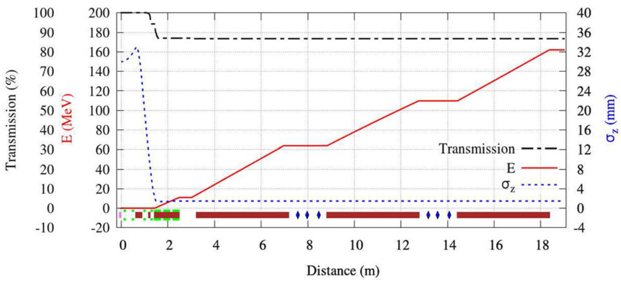

Fig. 3 (Color online) Beam energy, bunch length, and transmission rate evolution of a single bunch along the injector linac

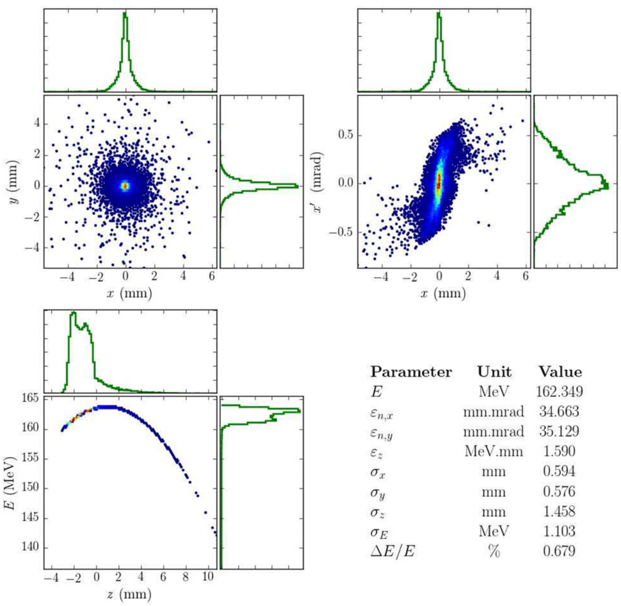

Parameter	Unit	Value
E	MeV	162.349
$\varepsilon_{n,x}$	mm.mrad	34.663
$\varepsilon_{n,y}$	mm.mrad	35.129
ε_z	MeV.mm	1.590
σ_x	mm	0.594
σ_y	mm	0.576
σ_z	mm	1.458
σ_E	MeV	1.103
$\Delta E/E$	%	0.679

Fig. 4 (Color online) Transverse beam distribution (top right is horizontal and top left is vertical), longitudinal phase spaces (bottom left), and the beam parameters of the bunch at the end of injector linac. The histograms associated with each macroparticle distribution show the projection along the respective axis

ring [10–13]. A long booster ring shares the same tunnel with the storage ring designed for TURKAY.

The circumference of the storage ring is 477.4 m. A reasonable tunnel space is needed to allow the installation of equipment, and it is found at least around 30 m difference in circumference is needed. Hence, the circumference of the booster is 445.6 m. With the 500 MHz RF frequency, the storage ring harmonic number is 795. The harmonic number of the concentric booster is 742 with the same RF frequency. The lattice of the booster ring is a combined function FODO lattice structure. There are eight superperiods, and each superperiod consists of six cells of a combined function FODO lattice and two matching cells. Each bending magnet used in the FODO cells are 1.5 m long with a bending angle of 5.625°, and they have defocusing quadrupole and sextupole field components. So, the dipole field is 0.65 T at 3 GeV and 0.033 T at 150 MeV. The quadrupoles provide the focusing strength, and they also include the focusing sextupole field components. The matching cell at the end of each superperiod consists of four matching quadrupoles and two combined function dipoles. The total bending angle of these two bending magnets is 5.625°. Also, the matching cells include pairs of extra sextupoles. The optical functions are shown in Fig. 5, and the basic parameters of the booster are listed in Table 2. The circumference of the booster ring is 445.6 m, and the lattice consists of 8 (4.8 m) straight sections with zero dispersion suitable for the installation of RF cavity, injection, and extraction systems. The emittance value of the ring at 3 GeV is 2.92 nm rad. OPA, ELEGANT, BEAMOPTICS, and MADX codes are used to design a magnetic lattice of booster rings [14–17].

Natural chromaticity should be corrected by the sextupole magnets. However, the nonlinearities of strong sextupole magnets affect the dynamic aperture, which is the transverse area of the particle in which it can execute its oscillations safely without getting defocused or lost. This is due to the quadratic field distribution in the sextupole magnets. The nonlinear forces on the particle which lead to anharmonic betatron oscillations arise and the particle loses above a certain amplitude. Particles with nominal momentum but wrong oscillations will be deflected by the sextupole fields, and it will no longer be possible to find a stable trajectory [18]. This effect can be compensated by the use of other sextupoles. The dynamic aperture, including synchrotron radiation effect for different momentum offsets at the injection point, is shown in Fig. 6. The beam sizes at injection are $\sigma_x = 0.82$ mm and $\sigma_x = 1.3$ mm. The dynamic aperture is large enough for the requirements of injection and extraction processes.

The condition for optical resonance in both planes is expressed as

$$mQ_x + nQy = p\,, \qquad (1)$$

where m, n, and p are integers and Q_x and Q_y are horizontal and vertical tunes. $m + n$ is the resonance order and is

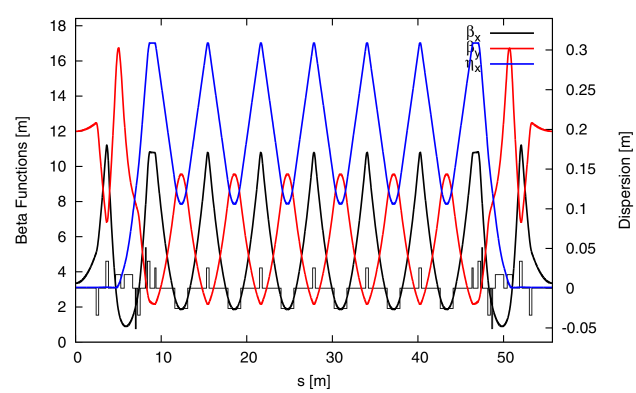

Fig. 5 (Color online) Optical functions in one superperiod of the booster ring

Table 2 The main parameters of the booster ring

Parameters	Value
Energy (GeV)	0.15–3.0
Circumference (m)	445.6
H. emittance (nm rad)	2.92
Energy loss/part./turn (3 GeV) (keV)	461.6
Max. β_x (m)	11.0
Max. β_y (m)	16.5
β_x in the mid. of straight sect. (m)	3.35
β_y in the mid. of straight sect. (m)	12
D_x in the mid. of straight sect. (m)	0.00
Betatron tunes Q_x/Q_y	30.85/13.92
Natural chromaticity ξ_x/ξ_y	− 29.63/− 20.18
Number of superperiods	8
Damping time H/V/Long. (ms)	10.680/19.323/16.228
Harmonic number	742

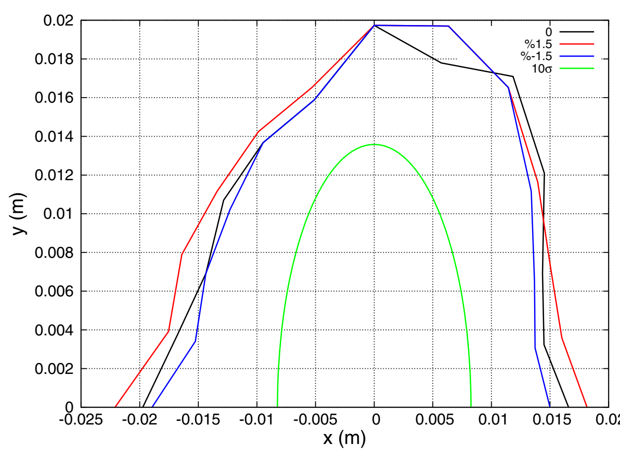

Fig. 6 (Color online) Dynamic aperture of the booster ring for different momentum offsets (magnet errors is zero, 10,000 turns)

generally concerned about resonances up to the fifth order. For stable operation, the horizontal and vertical tune values, named working point, should be chosen carefully, and they should be away from resonance lines. Frequency map analysis (FMA) [19] is a numerical method for understanding the effect of resonance on the dynamic aperture. For this purpose, the diffusion rate,

$$D = \mathrm{Log}_{10}\sqrt{\Delta v_x^2 + \Delta v_y^2}, \tag{2}$$

can be used as a stability index [20]. Δv_x and Δv_y are the transverse tune shifts of surviving particles in tracking. Figure 7 shows the frequency map of a single particle tracked by the code ELEGANT. As it is seen from the figure, especially in the central region of the aperture, the effect of the resonant is so limited.

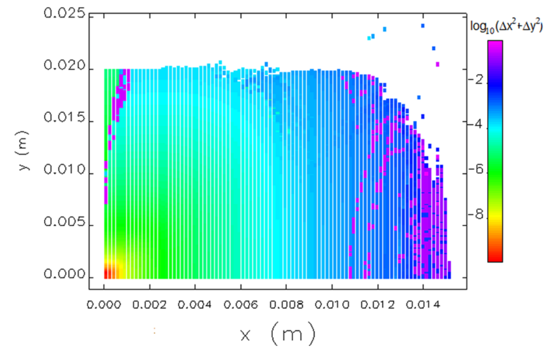

Fig. 7 (Color online) Frequency map of the booster obtained from tracking of two thousands turns

The misalignment and field errors of the magnets can be cause to the closed orbit distortion (COD) which is one of the error sources in the high-intensity synchrotron ring. The distortion can be corrected by the use of beam position monitors and horizontal and vertical correctors. Simulation results for distorted and corrected closed orbits are shown in Figs. 8 and 9, respectively. The errors applied to the magnets have a Gaussian distribution with a cutoff in three sigma and accepted misalignment deviations (displacement and roll of magnetic elements) as shown in the Table 3. The maximum corrector strength is limited to 1 mrad.

In a booster ring, the emittance and the energy spread change during acceleration. Time evolutions of the emittance and the energy spread during ramping is given by [21]

$$\frac{\mathrm{d}\varepsilon}{\mathrm{d}t} = -\frac{1}{\gamma(t)}\frac{\mathrm{d}\gamma(t)}{\mathrm{d}t}\varepsilon - \frac{2}{\tau_x}\varepsilon + \frac{1}{J_x}\frac{2}{\tau_x}C_q\gamma^2(t)\frac{I_5}{I_2}, \tag{3}$$

$$\frac{\mathrm{d}\sigma^2}{\mathrm{d}t} = C_q\gamma^2(t)\frac{2}{J_z\tau_z}\frac{I_3}{I_2} - \left(\frac{2}{\tau_z} + \frac{1}{\gamma(t)}\frac{\mathrm{d}\gamma(t)}{\mathrm{d}t}\right)\sigma^2, \tag{4}$$

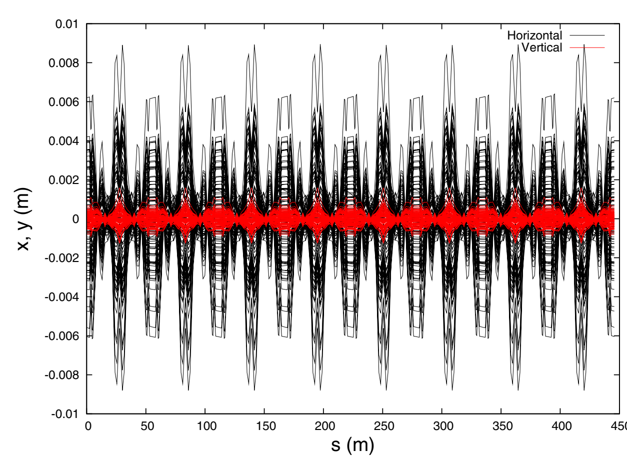

Fig. 8 (Color online) Closed orbit distortion along the booster ring for 100 seeds of random errors

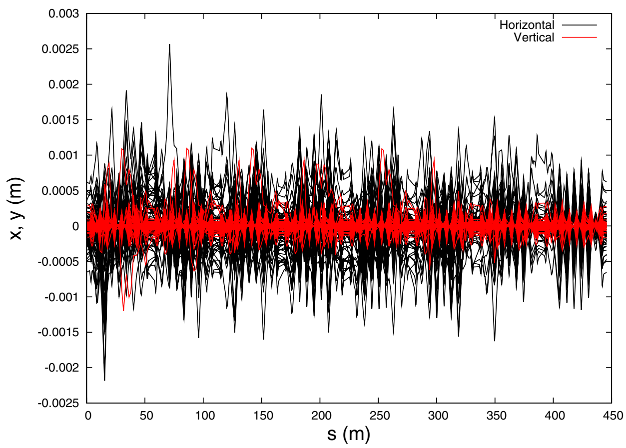

Fig. 9 (Color online) Corrected closed orbit along the booster ring for 100 seeds of random errors

Table 3 Deviations of the errors applied to the magnets of the booster ring

Error type	Dipoles	Quadrupoles	Sextupoles
Δx (mm)	0.2	0.2	0.2
Δy (mm)	0.2	0.2	0.2
$\Delta \phi$ (mrad)	0.5	0.5	0.5
Dipole field error (%)	0.1	–	–

where C_q is $3.832 \times 10^{-3}\,\mathrm{m/(GeV)^2}$, J_x and J_z are the partition numbers, τ_x and τ_z are the damping numbers, and I_2, I_3, I_5 are the synchrotron integrals. Evolution of the emittance and energy spread of the beam during the ramping from Eqs. (3) and (4) and particle tracking simulation with ELEGANT are shown in Fig. 10. The Fig. 11 shows the beam energy evolution and number of particles

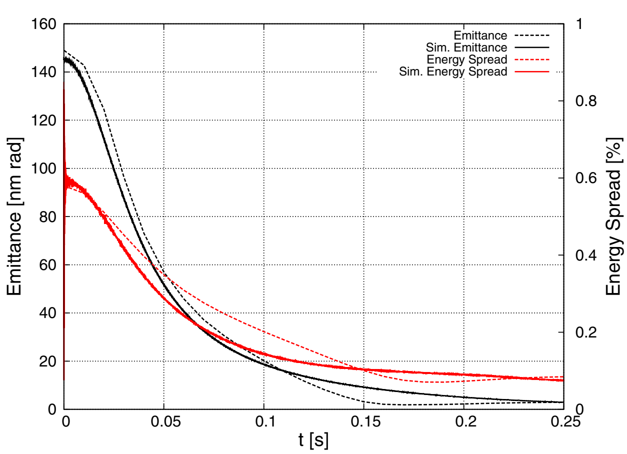

Fig. 10 (Color online) Time evolution of the beam emittance and energy spread during ramping in the booster

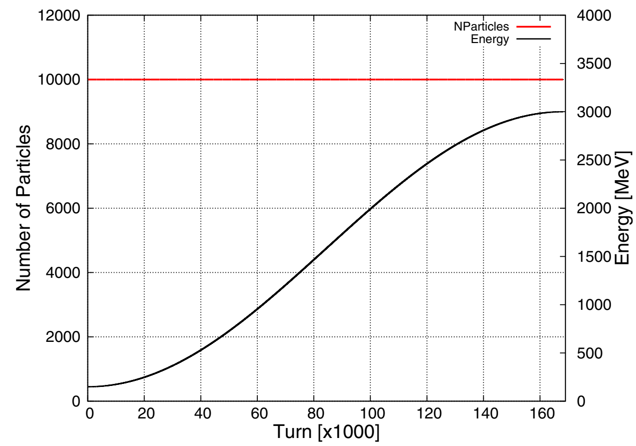

Fig. 11 (Color online) Energy evolution and number of particles during ramping in the booster

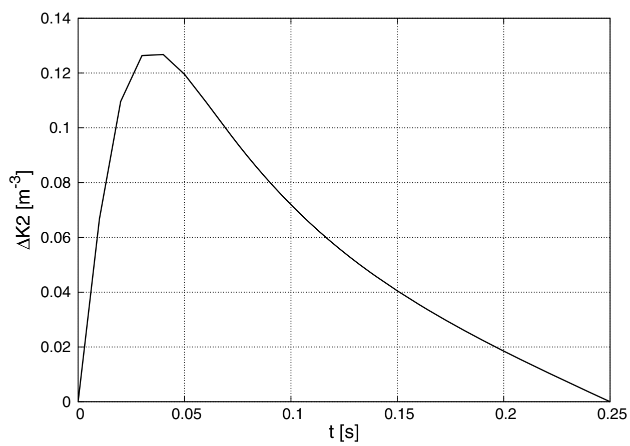

Fig. 12 (Color online) Eddy current induced sextupole field (2 Hz)

during the ramping from a tracking simulation with 10,000 particles. All particles survived in the acceleration process.

The variation of the magnetic field in the magnets, especially bending magnets, will induce an eddy current, and as a result, a sextupole field occurs in this region. Due to this sextupolar gradient, the chromaticity of the ring will change during the ramping. This effect is investigated for an elliptic stainless steel vacuum chamber 1 mm thick. The evolution of the sextupole field and chromaticity during the ramping are shown in Figs. 12 and 13. The effect of the eddy current is maximum at 0.04th second. The chromticities can easily be corrected with two lattice sextupole families.

5 Linac to booster transfer lines

The linac to booster (LTB) transfer line consists of 2 bending magnets, 1 septum, 1 kicker magnet, and several quadrupoles for optical matching. The bending angle of the

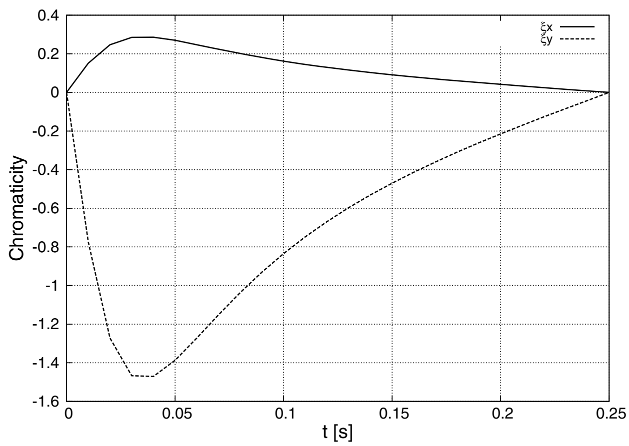

Fig. 13 (Color online) Chromaticities induced by eddy currents on the dipoles vacuum chambers due to the ramping process

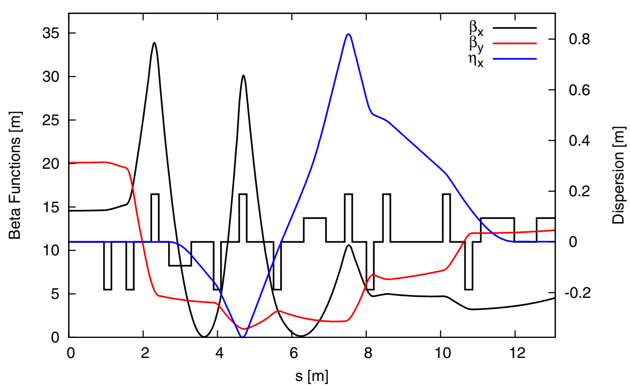

Fig. 14 (Color online) Optical parameters of the linac to booster transfer line

septum is 10°, and the kick angle of the kicker magnet is 1°. Figure 14 shows the optical functions along the LTB transfer line. The horizontal and vertical betatron values are matched to the parameters of the injection point of the booster. The maximum betatron functions are controlled within 35 m under the constraints of well dispersion matching. Maximum beam sizes along the line are $\sigma_x = 5$ mm and $\sigma_y = 2.3$ mm. The beam stays clear which determines the vacuum chamber size is defined as 3σ of the beam size and 5 mm tolerance for the trajectory distortion. Therefore, the aperture requirements are ± 20 mm horizontal and ± 15 mm vertical. Figure 15 shows the beam phase spaces from the particle tracking simulation in injection. According to the simulation results, 100% transmission is achieved.

There are two methods for injection from the booster into the storage ring. First, off-axis injection with an orbit bump generated by several kicker magnets. Second, on-axis injection with a single nonlinear kicker, as developed recently at BESSY II [22]. For top-up injection, the second process can be very helpful to minimize residual beam excitation by the injection process. The design study for the booster to the storage ring transfer line continues, and the injection process is under discussion.

6 Summary

In this paper, we have described the design of the beam dynamics of the TURKAY injector. Each component of the injector linac, such as solenoids and RF structures are preliminary designed in order to make proper simulation with the ASTRA code. Simulations show that the injector linac can deliver more than 85% of particles to the booster within the requested parameters of the booster ring. However, no static or dynamic imperfections has been taken into account during the simulation of pre-injector linac at present. In the presence of the imperfections, such as RF and magnet errors, the efficiency is expected to be more than 75%. It will be studied in detail in the next stage of the work. An eightfold symmetry booster ring is in design, and this ring will share the same tunnel with storage ring. Top-up injection is nowadays state of the art for storage ring-based SR sources. For radiation safety reasons, the electron beam losses during injection with open photon beam shutters have to be minimized. Therefore, the booster emittance should be small to capture the full beam in the storage ring acceptance. The 2.92 nm rad horizontal emittance is sufficiently low for this purpose. The tracking simulations show that the particles can be ramped to 3 GeV nominal energy without particle looses.

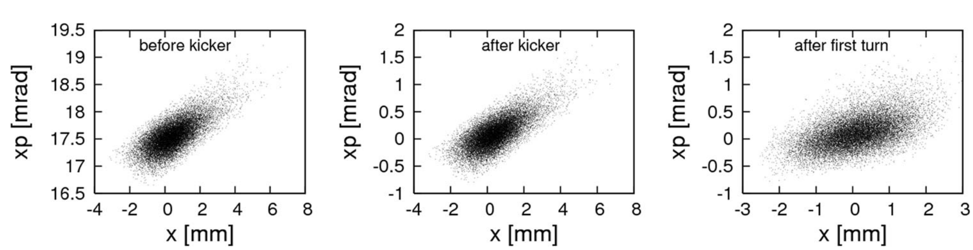

Fig. 15 Phase spaces of the injected beam to the booster after and before the kicker magnet and after first turn at the booster (reference point is the kicker in the coordinate of the booster)

References

1. S. Sultansoy, M. Yilmaz, O. Cakir et al., The status of Turkic accelerator complex proposal, in *Proceedings of PAC05* (Knoxwille, TN, USA, 2005), p. 449. doi:10.1109/PAC.2005.1590465
2. A. Aksoy, Ö.Yavaş Ö Karslı, The Turkish accelerator complex IR FEL project. Infrared Phys. Technol. **51**, 378–381 (2008). doi:10.1016/j.infrared.2007.12.027
3. A. Aksoy, U. Lenhert, Beam transport and bunch compression at TARLA. Nucl. Instrum. Methods A **762**, 54–63 (2014). doi:10.1016/j.nima.2014.05.107
4. Z. Nergiz, Radiation properties of Turkish light source facility. Nucl. Instrum. Methods A **795**, 140–143 (2015). doi:10.1016/j.nima.2015.05.068
5. Z. Nergiz, A. Aksoy, Low emittance lattice for the storage ring of the Turkish Light Source Facility TURKAY. Chin. Phys. C **39**(6), 067002 (2015). doi:10.1088/1674-1137/39/6/067002
6. M. Pont, G. Benedetti, J. Moldes et al., Top-up operation at ALBA Synchrotron Light Source, in *Proceedings of IPAC14* (Dresden, Germany, 2014)
7. H. Ohkuma, Top-up operation in light sources, in *Proceedings of EPAC08* (Genoa, Italy, 2008), p. 36
8. M. Pont, D. Eindeld, A. Falone et al., Status of the 100 MeV Preinjector for the ALBA Synchrotron, in *Proceedings of EPAC08* (Genoa, Italy, 2008)
9. K. Floettmann, ASTRA User Manual (2011)
10. G. Benedetti, D. Eindeld, Z. Marti et al., Optics for the ALBA Booster Synchrotron, in *Proceedings of EPAC08* (Genoa, Italy, 2008), p. 2148
11. C.C. Kuo, H.P. Chang, H.C. Chao et al., Accelerator physics issues for TPS, in *Proceedings of IPAC10* (Kyoto, Japan 2010), p. 36
12. A.R.D. Rodrigues, F. Arroyo, O.R. Bagnato et al., *SIRIUS Design Report*. Technical Report, LNLS, Campnas Brasil (2013)
13. H. Ghasem, H. Ahmadi, Conceptual design and expected performance of Iranian light source facility injectors. Nucl. Instrum. Methods A **795**, 228–238 (2015). doi:10.1016/j.nima.2015.05.034
14. A. Streun, OPA version 3.39 PSI, March 14 (2012)
15. M. Borland, *Elegant: A Flexible SDDS-Compliant Code for Accelerator Simulation*. Technical Report, Advanced Photon Source (2000)
16. H. Grote, F. Schmidt, The MAD-X Program. http://mad.web.cern.ch
17. H. Wiedemann, BEAMOPTICS, Applied Physics Department, Stanford University
18. K. Wille, *The Physics of Particle Accelerators* (Oxford University Press, Oxford, 1996). p.123
19. J. Laskar, Introduction to the frequency map analysis, in *NATO Advanced Study Institute*, ed. by C. Simo (Kluwer, Dordrecht, 1999)
20. L. Nadolski, J. Laskar, Review of single particle dynamics for third generation light sources through frequency map analysis. Phys. Rev. Spec. Top-AC **6**, 114801 (2003). doi:10.1103/PhysRevSTAB.6.114801
21. A. Wolski, *Low-Emittance Machines* (CAS, Daresbury, UK, 2007)
22. T. Atkinson, M. Dirsat, O. Dressler et al., Development of a nonlinear kicker system to facilitate a new injection scheme for the BESSY II storage ring, in *Proceedings of IPAC2011* (San Sebastian, Spain, 2011), p. 3394